Proceedings of ASME Turbo Expo 2010: Power for Land, Sea and Air
GT2010
June 14-18, 2010, Glasgow, UK

GT2010-22082

THE INFLUENCE OF TIP CLEARANCE ON THE ACOUSTIC AND AERODYNAMIC CHARACTERISTICS OF FANS

Sascha Karstadt
Chair of Fluid Systems Technology
Technische Universität Darmstadt
Darmstadt, Germany
Email: Sascha.Karstadt@fst.tu-darmstadt.de

Michael Hess
Chair of Fluid Systems Technology
Technische Universität Darmstadt
Darmstadt, Germany
Email: Michael.Hess@fst.tu-darmstadt.de

Berthold Matyschok
Chair of Fluid Systems Technology
Technische Universität Darmstadt
Darmstadt, Germany
Email: Berthold.Matyschok@fst.tu-darmstadt.de

Peter F. Pelz*
Chair of Fluid Systems Technology
Technische Universität Darmstadt
Darmstadt, Germany
Email: Peter.Pelz@fst.tu-darmstadt.de

ABSTRACT

In addition to developing fans as aerodynamically efficient as possible, acoustic gains more and more importance for the purpose of reducing fan noise exposure. In order to combine good aerodynamic properties with a silent fan, this experimental research investigates the acoustic and aerodynamic characteristics of an axial fan. In this case, a fan with skewed blades is tested in view of its aerodynamic efficiency and noise exposure in dependence on its tip clearance and stagger angle. For this purpose, six different stagger angles and five tip clearance gaps per angle were measured in a fan test rig (according to ISO 5136). Interpretation of the recorded data shows a clear trend toward higher aerodynamic efficiency and less noise with a down-sizing of the tip clearance gap. As the cost of manufacture rises with the decrease of the tip clearance, the efficiency of these measures can be calculated with the results of this study under consideration of aerodynamic and acoustic aspects.

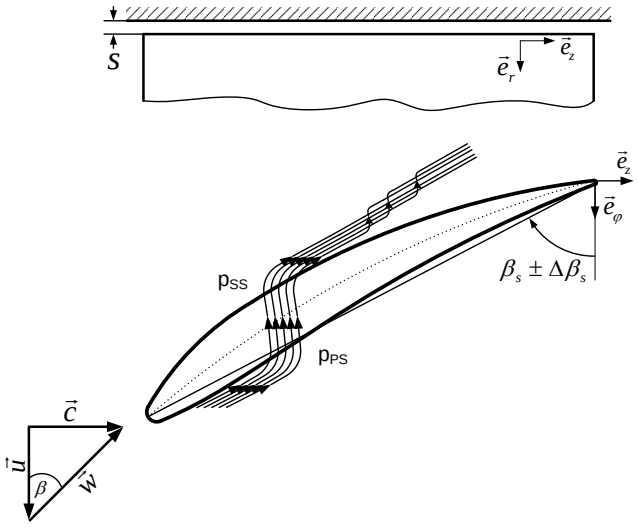

Figure 1. TIP CLEARANCE AND TIP LEAKAGE FLOW

INTRODUCTION

Nowadays the dimensions of manufactured fans vary from small radial fans of several millimeter in diameter for cooling

*Address all correspondence to this author.

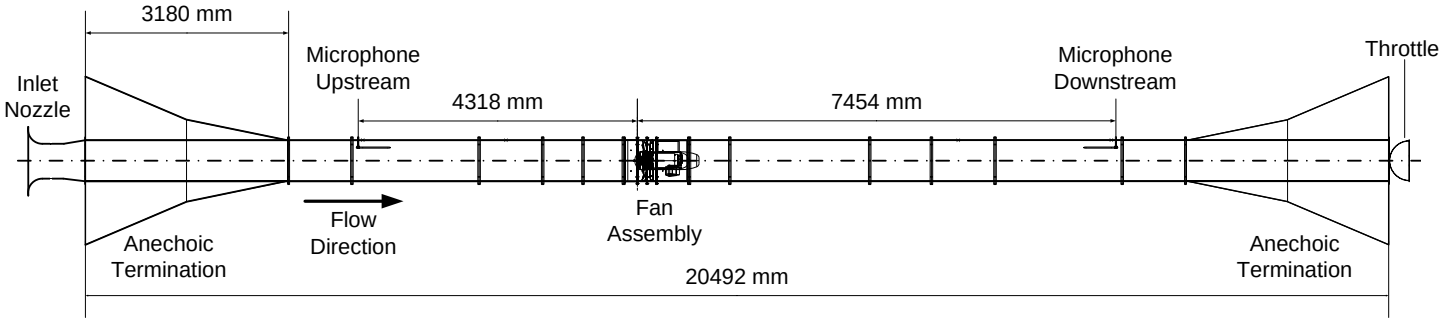

Figure 2. SKETCH OF THE TEST RIG

NOMENCLATURE

A_D	Duct cross sectional area
A_R	Ring cross sectional area
D	Inner duct diameter
D_i	Hub diameter
D_o	Outer fan diameter
K	Calibration coefficient
$\overline{L_p}$	Corrected sound pressure level
L_w	Sound power level
$L_{w,spez}$	Specific sound power level
M	Torque
$\dot{V}$	Volume flow rate
Re	Reynolds number
c	Speed of sound
f	Frequency
n	Rotational speed
p_d	Dynamic pressure
p_s	Static pressure
p_t	Total pressure
s	Tip clearance

Greek symbols

Δp_D	Static pressure difference
Δp_{sys}	Blowing out pressure difference
Δp_t	Total pressure difference
Δp_K	Static pressure difference
$\Delta\beta_s$	Stagger angle
$\Delta\eta_{sys,max}$	Difference in maximum efficiency
β_s	Design angle
η_{sys}	System efficiency
$\eta_{sys,max}$	Maximum system efficiency
η	Efficiency with total pressure rise
ν	Hub-tip ratio
ρ	Air density
τ	Relative tip clearance
φ	Flow coefficient
ψ	Pressure coefficient

computer chips to huge axial fans in wind tunnels which can reach more than 15 m in diameter. Additionally to the continuing improvement of aerodynamic efficiency, in recent years research attached great importance to reducing the noise emission of turbo-machines. In the field of gaining quieter fans good progress was made by developing skewed blades, for example. In [1] it was shown that for skewed blades the aerodynamic performance as well as the emitted sound power level improves. Beside the further development of the blades, it is increasingly attempted to further raise the aerodynamic efficiency and reduce sound generation by optimizing the stationary devices e.g. the casing of the turbo-machine. One possibility is to design the tip clearance s between the rotor blades and the casing so that a good compromise for efficiency and noise emission as well as manufacturing costs can be found. Improvement of the casing in order to get smaller tip clearances increases the manufacturing cost in consequence of tighter tolerances for both - rotating and stationary parts.

To investigate the influence of tip clearance on the aerodynamic and acoustic characteristics of a fan a test rig was constructed and built. Because of the tip clearance and due to a pressure difference between the suction and the pressure side of the blade a tip-leakage flow is formed (Fig. 1). The intensity of the tip-leakage flow and the related tip-leakage vortex depends on the size of the gap and the pressure difference between the pressure and the suction side of the blades. In the limit $s/D_o \to 0$ no tip leakage vortex is formed. According to the Helmholtzs vortex theorems the leading edge vortex in this case would reach infinite radius. In the limit $s/D_o \to \infty$ (no casing) the tip leakage vortex is of the same strength as the leading edge vortex. As shown in [2] in 1926 this secondary flow has, in addition to the losses in pressure, an influence on the blades incident flow and causes separation at the blade tips, which leads to an earlier start of the rotating stall with increasing tip clearance. In order to quantify the aerodynamic losses and the acoustic changes, caused by the flow and the vortex, five tip clearances and six stagger angles were tested and analyzed. The aerodynamic losses caused by the tip clearance are regarded in differences of total pressure loss which also lead to minor aerodynamic efficiencies. The higher noise emission is shown in the change of sound power level. Also changes within the frequency spectrum are regarded.

Earlier studies from Marcinowski in 1958 [3] and Kameier in

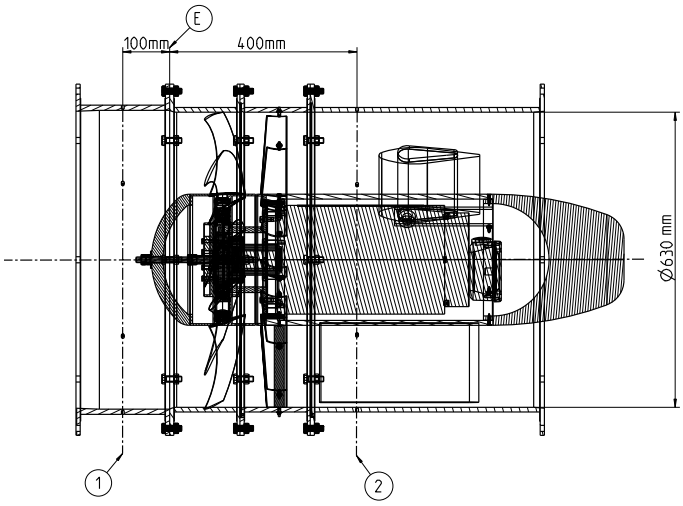

Figure 3. FAN ASSEMBLY

1993 [4] also analyzed the influence of the tip clearance. Marcinowksi specified the difference of the highest reachable system efficiency $\eta_{sys,max}$ from the relative tip clearance $\tau = 0.1\%$ to $\tau = 0.8\%$ for an eight-bladed fan to $\Delta\eta_{sys,max} \approx 0.13$. In this study τ is always the relative tip clearance s/D_a. The change in the sound emission of the fan was also tested and a shift of the peak, caused by the tip clearance noise, towards smaller frequencies with increasing tip clearance was detected. In literature and this study tip clearance noise specifies the peaks in the frequency spectrum which are generated while enlarging the tip clearance. Kameier gives a value of $\Delta\eta_{sys,max} \approx 0.07$ for an increasing tip clearance from $\tau = 0.066\%$ to $\tau = 0.53\%$ for a 24-bladed fan with a hub-tip ratio $\nu = D_i/D_o = 0.62$. The rise of the specific sound power is related to a broadband increase of the sound pressure level with a discrete rise and movement of the peak caused by the tip clearance noise. This was also found by Fukano and Jang [5]. They showed that the frequency related to this this peak matches approximately with the period of one rotation of the tip-clearance vortex. They also showed that the frequency shift of the peak depends on the flow coefficient φ (Eqn. 2), the size of the tip clearance s and the rotational speed of the fan n, which could be affirmed by this study.

EXPERIMENTAL SETUP AND METHODOLOGY

The experiments were performed in a fan test rig according to ISO 5136 [6] located at the laboratory of the Chair of Fluid Systems Technology at Technische Universität Darmstadt [7]. This standard defines the required setup to measure and compare the emitted acoustic power of fans and other turbo-machines. In this test case a fan with nine skewed blades, 13 guide vanes, an outer diameter of $D_o = 0.63$ m and a hub-tip ratio of $\nu = 0.45$ was mounted on the test rig. The blades have a backward sweep in the hub and a forward sweep in the tip region. They were designed using a free vortex design method with constant total pressure rise across the span of the fan blade. As shown in Fig. 3, the fan assembly is partitioned into rings with different inner diameters which can easily be replaced to vary the tip clearance. The inner diameter of the flow path segments upstream and downstream of the rotor is designed in a way that even with the ring used for the largest tip clearance there is always a reduction in the cross sectional area. This always leads to an accelerated flow, where round edges at the occurring steps additionally ensure, that there is no flow separation. For this study the tip clearances were $\tau = 0.1\%, 0.2\%, 0.3\%, 0.5\%$ and 0.8% of the outer fan diameter. The variation of the stagger angle ($\Delta\beta_s = 12°, 6°, 0°, -6°, -12°, -18°$) was realized with six sets of blades. Each set was trimmed separately in its mounted position in order to get a constant gap over the cord length. During the experiments the rotational speed was $n = 41.66$ 1/s to achieve a constant Reynolds number of $Re = \pi n D_o^2/\nu = 3.5 \cdot 10^6$ with the kinematic viscosity $\nu = 15 \cdot 10^{-6}$ m^2/s for air at standard conditions. A throttle at the pressure side end of the test rig was used to vary the volume flow rate $\dot{V}$ by changing counter pressure.
For every characteristic in the average 19 points were measured. The first point of every characteristic was measured with the throttle completely open, so that the volume flow was at its maximum. For the following points the flow was throttled until the fan reached the stall region. The last measured point was not yet at stall conditions.

Volume Flow Rate

Measurement of the volume flow rate is performed with an inlet nozzle. The static pressure difference between the ambient and the accelerated flow inside the nozzle with a calibration coefficient K is used to calculate the air speed at a given area. In case of the used inlet nozzle K is constant and the volume flow rate can be calculated to $\dot{V} = K\sqrt{\frac{\Delta}{p}_D/\rho}$. The six pressure measure locations distributed over the circumference of the inlet nozzle are connected by a circular manifold, to connect and average the pressure.

Pressure

Pressure measurements are made with a 16 channel scanner by Pressure Systems. Calibration allows that the 16 channels can be measured simultaneously with an absolute uncertainty of less than 1 Pa. The total pressure rise of the fan is ascertained by two static pressure measurements. Figure 3 shows two measuring planes - 1 and 2.In each plane there are six static pressure drills. Knowing the volume flow rate and the static pressure difference over the fan stage $\Delta p_K = p_2 - p_1$ the total pressure rise can be

calculated by

$$\Delta p_t = p_{t_2} - p_{t_1} = \Delta p_K + \frac{\rho}{2}\left(\frac{\dot{V}}{A_R}\right)^2\left[1-\left(\frac{A_R}{A_D}\right)^2\right]. \quad (1)$$

The dynamic pressure is determined by the volume flow rate. A_D denotes the circular cross sectional area of the duct. A_R describes the ring cross sectional area at plane 2. Due to the guide vanes behind the rotor there is only negligible swirl at plane 2. The same is true for plane 1.

Torque

To determine the aerodynamic efficiencies of the fan an input power has to be obtained. Therefore a flying mounted torque flange manufactured by Manner Sensortelemetrie was installed between the driveshaft and the fan. Due to the direct installation at the rotor the torque M is measured without any bearing friction torque. Because of the small surface, disc friction torque is negligible compared to the aerodynamic torque.

Dimensionless Products

In order to allow comparisons with other turbo-machines the characteristic curves are always plotted with dimensionless products. As mentioned above the dimensionless flow rate is the flow coefficient

$$\varphi = \frac{4\dot{V}}{n\pi^2 D_o^3}. \quad (2)$$

The dimensionless total pressure rise is given in form of the pressure coefficient

$$\psi = \frac{2\Delta p_t}{\rho\left(n\pi D_o\right)^2}. \quad (3)$$

With measured torque M and the rotational shaft speed n, the efficiency of the fan can be determined to:

$$\eta = \frac{\dot{V}\Delta p_t}{2M\pi n}. \quad (4)$$

If the system efficiency of a fan blowing out directly in the ambient is considered, this efficiency is of course smaller than Eqn. (4) since the mixed out loss $\rho/2\left(\dot{V}/A_R\right)^2$ has always to be overcome. The system efficiency for blowing out directly after the fan can then be calculated by

$$\eta_{sys} = \frac{\dot{V}\Delta p_{sys}}{2M\pi n}, \quad (5)$$

with $\Delta p_{sys} = \Delta p_t - p_{d_2}$.

Uncertainty of Measurement

The uncertainty of measurement for φ is in the range of 1-1.3 % based on the actual volume flow. For η the uncertainty is smaller than 1.2 %, for η_{sys} smaller than 1 % absolute efficiency, according to actual pressure rise, volume flow rate and torque.

Sound

The sound within the duct is measured with two microphones each close to the anechoic terminations at the ends of the duct. The microphones are installed approximately 7 times the inner duct diameter D upstream, and approximately 11 times D downstream of the reference plane E (Fig. 2). The pressure field microphones are manufactured by Bruel & Kjaer with a recordable frequency range between 3.15 Hz and 20 kHz. In this study the analyzed frequency range expends from 16 Hz to 16 kHz. Every item in the duct which is exposed to the turbulent flow generates a noise. The microphones are installed in a turbulence screen to generate a minimal and known background noise at known frequencies, depending on the flow rate, which can be eliminated in later calculations. With a two-channel microphone amplifier, the acoustic signals are recorded and analyzed with a computer. The sound power level used in this study is determined in decibel (dB) according to [6]:

$$L_w = \overline{L_p} + \left[10\,lg\frac{A_K}{A_0} - 10\,lg\frac{\rho c}{(\rho c)_0}\right], \quad (6)$$

where $A_0 = 1$ m^2 is a reference cross sectional area and $(\rho c)_0 =$ 400 Ns/m^3 is the acoustic impedance at standard conditions. $\overline{L_p}$ is the corrected sound pressure level determined according to [6]. In order to be able to compare fans at different operating points [8] introduced the specific sound power

$$L_{wspez} = L_w + \left(10\,lg\dot{V} - 20\,lg\Delta p_t\right), \quad (7)$$

which will be used in this study.

RESULTS

All points shown in this study are measured with the described measurement technique while the lines are interpolated with a 5th degree polynomial, with the exception of Fig. 8, Fig. 15 and plots with the frequency spectrum.

Aerodynamics

Figure 4 shows the aerodynamic characteristics, pressure coefficient ψ versus the flow coefficient φ of the tested fan for a

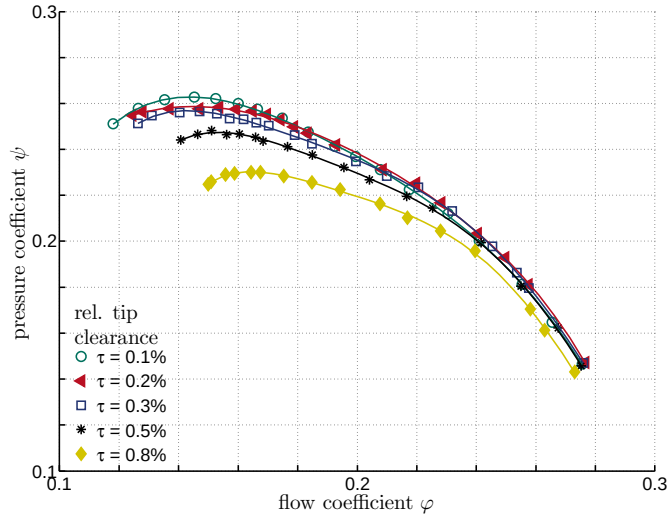

Figure 4. AERODYNAMIC CHARACTERISTICS FOR $\Delta\beta_s = 0°$

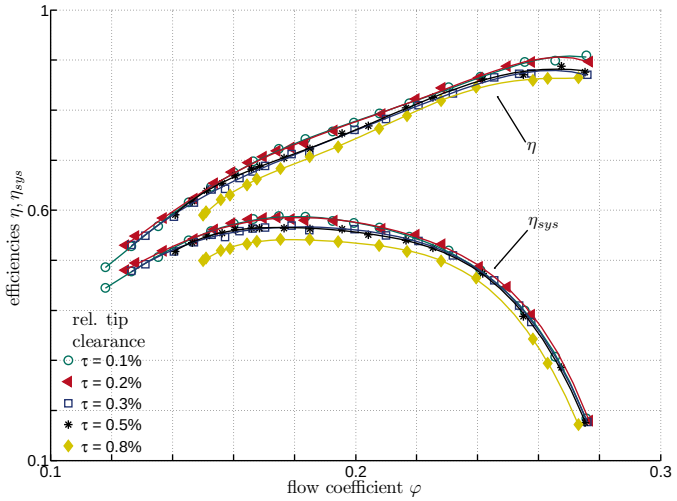

Figure 5. AERODYNAMIC EFFICIENCIES FOR $\Delta\beta_s = 0°$

stagger angle $\Delta\beta_s = 0°$ and the five tip clearances ranging from 0.1% to 0.8%. It is evident that with increasing tip clearance the pressure coefficient decreases. This is the consequence of larger tip-leakage flows over increasing blade tip clearances. The bigger difference for smaller flow coefficients is caused by a higher pressure difference between the pressure and the suction side of the blades at higher pressure coefficients.
The point with the lowest flow coefficient of each curve is always the last stable point before the fan reaches the rotating stall region. For an increasing tip clearance the rotating stall starts at higher flow coefficients, so that the stable range of the fan be-

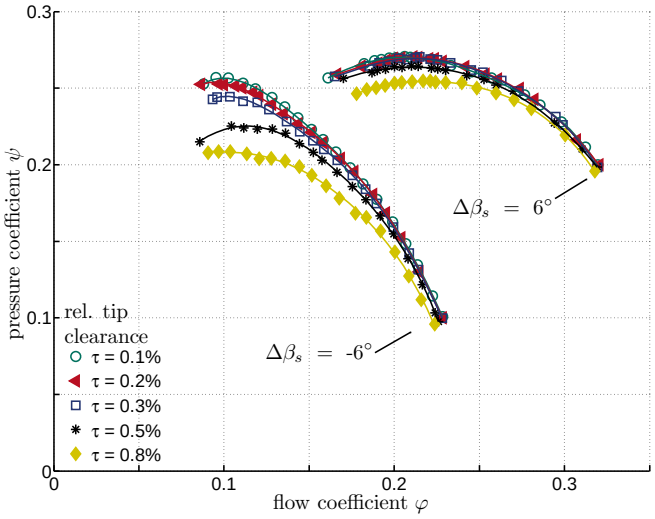

Figure 6. AERODYNAMIC CHARACTERISTICS FOR $\Delta\beta_s = 6°$ AND $\Delta\beta_s = -6°$

comes smaller. This is a sign of an influence of the tip clearance flow on the incident flow at the blade tips leading to separations in this operating range.
In Fig. 5 the aerodynamic efficiency η and the system efficiency η_{sys} calculated with Eq. 4 and 5 are shown. The relation between the system efficiency η_{sys} and the aerodynamic efficiency η is:

$$\eta_{sys} = \eta \left[1 - \frac{1}{(1-\nu^2)^2} \frac{\varphi^2}{\psi} \right] \tag{8}$$

Because the fan is not able to reach the peak operating point of aerodynamic efficiency η with the given test rig, this study from now on always focuses on η_{sys}. The biggest influence of tip clearance excluding the biggest gap with approximately 0.045 difference in the efficiencies, can be found in the region around the efficiency peak.

Figure 6 shows the aerodynamic characteristics for $\Delta\beta_s = 6°$ and $\Delta\beta_s = -6°$. It is obvious that, while the array of curves for $\Delta\beta_s = 6°$ is at a higher pressure level, the influence of the tip clearance is smaller. The efficiency for $\Delta\beta_s = 6°$ in Fig. 7 shows that although Δp_t and $\dot{V}$ are larger, peak η_{sys} is clearly lower. The difference of $\eta_{sys,max}$ between $\tau = 0.2\%$ and $\tau = 0.8\%$ is about $\Delta\eta_{sys,max} \approx 0.03$. Although the difference is in the range of the error in measurement, it can be seen that for $\Delta\beta_s = 6°$ and $\Delta\beta_s = -6°$ the smallest tip clearance does not have the largest efficiency. It can again be seen that the difference in efficiency caused by the larger tip clearance gets maximal for the efficiency peak. For $\Delta\beta_s = -6°$ and $\tau = 0.3, 0.5, 0.8\%$ a total stall could

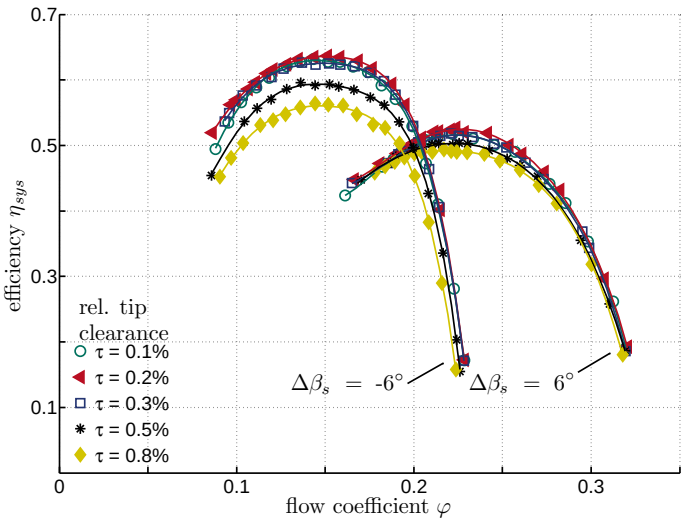

Figure 7. AERODYNAMIC EFFICIENCIES FOR $\Delta\beta_s = 6°$ AND $\Delta\beta_s = -6°$

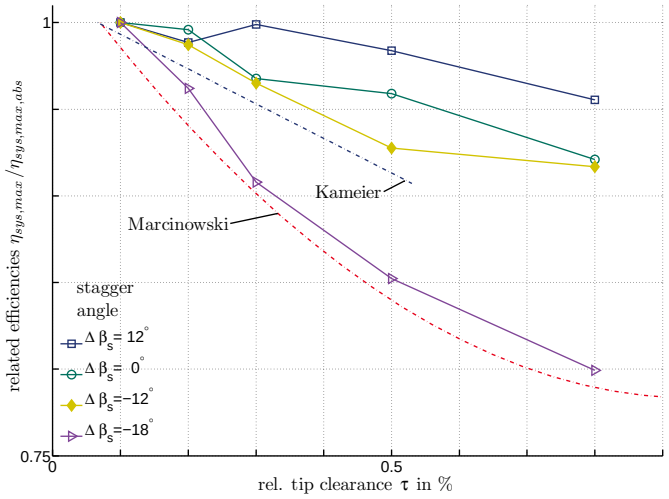

Figure 8. INFLUENCE OF RELATIVE TIP CLEARANCE ON AERODYNAMIC EFFICIENCIES

not be produced with the throttle at the end of the duct. For $\Delta\beta_s = -12°$ and for $\Delta\beta_s = -18°$, a total stall could not be generated for any tip clearance. Therefore no conclusion about the stable operating range of theses configurations could be drawn.

In Fig. 8 the influence of the tip clearance is shown by means of the peak efficiency for one tip clearance gap, based on the efficiency of $\tau = 0.1\%$ for this stagger angle. For clarity only four of six stagger angles and curves calculated out of Marcinowski [3] and Kameier [4] are plotted. Only about 92% of the peak efficiency is reached with $\tau = 0.8\%$ and a stagger angle $\Delta\beta_s = 0°$. The large negative gradient of the curve of Marcinowski can only be rudimentarily affirmed with $\Delta\beta_s = -18°$. In this study the maximal reached efficiency with $\Delta\beta_s = -18°$ and $\tau = 0.8\%$ was only $\approx 80\%$ of the value for $\tau = 0.1\%$. Although the largest tip clearance measured by Kameier is $\tau = 0.53\%$ the tendency of this curve fits better with the results of this study. It can also be determined that the influence is smaller for positive than for negative stagger angles. The influence between $\tau = 0.1\%$ and $\tau = 0.2\%$ is only about one per cent for all stagger angles except for $\Delta\beta_s = -18°$.

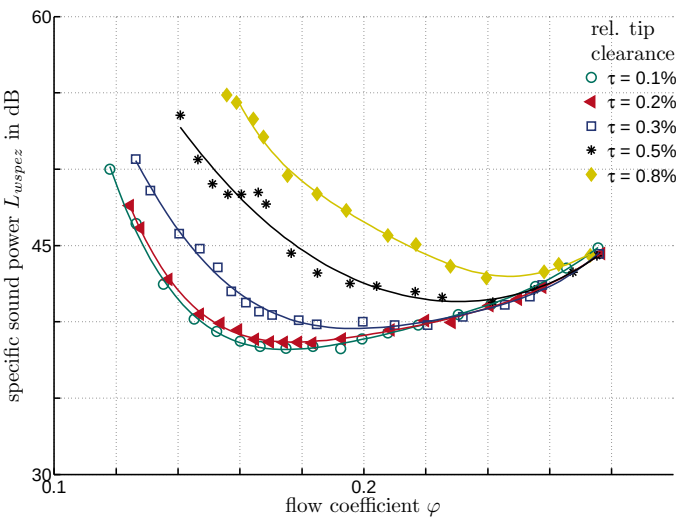

Figure 9. SPECIFIC SOUND PRESSURE POWER VERSUS FLOW COEFFICIENT FOR $\Delta\beta_s = 0°$

Acoustics

In Fig. 9 the specific sound power level is plotted versus the flow coefficient for fixed stagger angle $\Delta\beta_s = 0°$ but different tip clearances. The curves for $\tau = 0.1\%$ in Fig. 5 and Fig. 9 show a local minimum in noise generation an a local maximum in η_{sys} at the same flow coefficient. Because of the sound mainly generated by seperations caused by incident, the emitted sound rises off the optimum. With smaller flow coefficients the tip clearance vortex and later separations also contribute more to noise generation. This matches with the results Fukano and Jang show in [5] that the intensity of the tip-clearance vortex rises while throttling the flow rate. The tip-clearance vortex grows, the rotating frequency and the noise peak frequency decreases, which can also be confirmed with the results in this research. In [9] it was detected that with decreasing flow rate the tip leakage vortex is moving upstream and can interfere with the trailing edge of the following blade. This is disturbing the wake flow near the blade tip and generates noise. While increasing the flow rate the

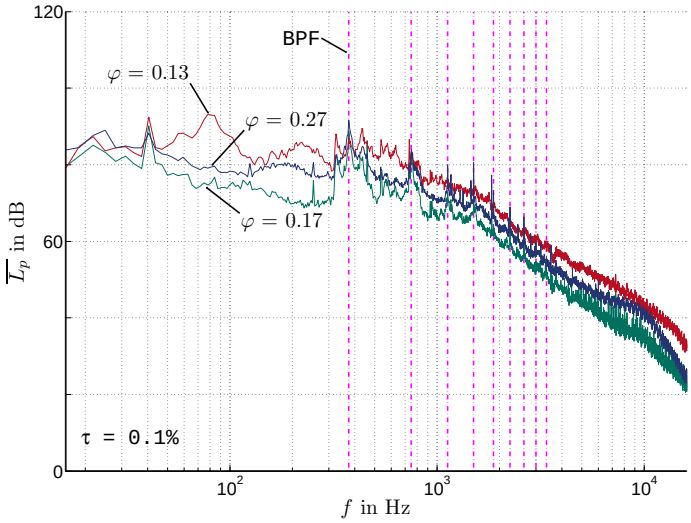

Figure 10. CORRECTED SOUND PRESSURE LEVEL VERSUS FREQUENCY FOR $\Delta\beta_s = 0°$ AND $\tau = 0.1\%$

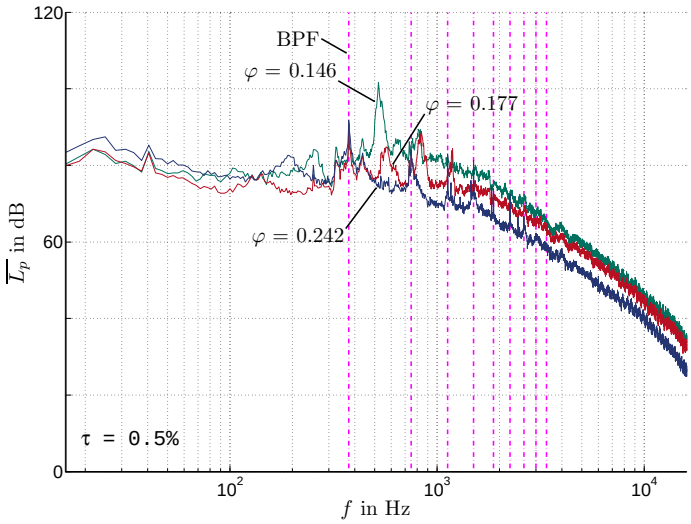

Figure 11. CORRECTED SOUND LEVEL VERSUS FREQUENCY FOR $\Delta\beta_s = 0°$ AND $\tau = 0.5\%$

tip leakage vortex interfaces with the suction side which results in high velocity fluctuation and again in higher noise emissions. In Fig. 10 the corrected sound power level is plotted versus the frequency for three operating points of the lowest curve in Fig. 9 with $\Delta\beta_s = 0°$ and a tip clearance of $\tau = 0.1\%$. The peak at $f = 41.66$ Hz results from a sound generated by the engine with a rotational speed $n = 41.66$ 1/s, but it was proved that the influence on the calculated sound power was neglectable. The peak at $f = 375$ Hz is called the Blade Passing Frequency (BPF) and

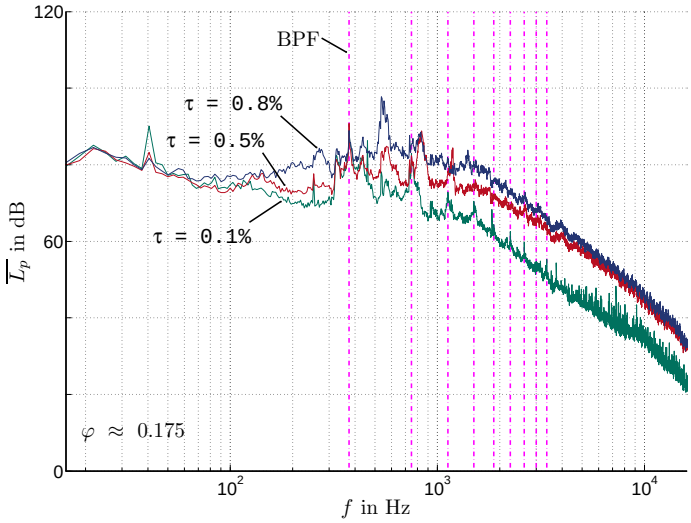

Figure 12. CORRECTED SOUND PRESSURE LEVEL VERSUS FREQUENCY FOR $\Delta\beta_s = 0°$

is defined as the product of the rotational shaft speed and the number of rotor blades. In the plot, the BPF and its harmonics are marked with dashed vertical lines. It can be seen that the increase of the specific sound power shown in Fig. 9 is caused by a rise of the corrected sound level over the whole frequency range. With smaller flow coefficients the regions of the clearance noise can also be seen slightly before and between the BPF and its first harmonic.

Figure 11 shows 3 operating points for $\Delta\beta_s = 0°$ and a tip clearance of $\tau = 0.5\%$.A broadband and discrete rise of $\overline{L_p}$ can be determined for decreasing flow coefficients. It can be seen more clearly that with smaller flow coefficients the tip clearance noise again rises between the BPF and its first multiple.

Regarding Fig. 9 it can be seen that with increasing τ the minimum of the curves are shiftet towards higher flow coefficients. Except for large flow coefficients the specific sound power increases strongly with increasing tip clearance. This can again be traced back to the increasing pressure difference between the suction and the pressure side of the blade. The difference in the specific sound power between $\tau = 0.1\%$ and $\tau = 0.8\%$ at an operating point with $\varphi \approx 0.175$ is about 12 dB. In Fig. 12 the corrected sound level for these points and $\tau = 0.5\%$ at nearly the same operating point is shown. As in [5] and [10] the increase of L_{wspez} is caused by a broadband and discrete rise of $\overline{L_p}$. The discrete rise mainly takes place before and between the BPF and its first two harmonics. Fukano and Jang in [5] as well as Kameier in [4] noticed a slight move of the peak caused by the tip clearance noise towards smaller frequencies when increasing the tip clearance. For this fan configuration the tip clearance noise is located mainly between the BPF and its first harmonic. A smaller

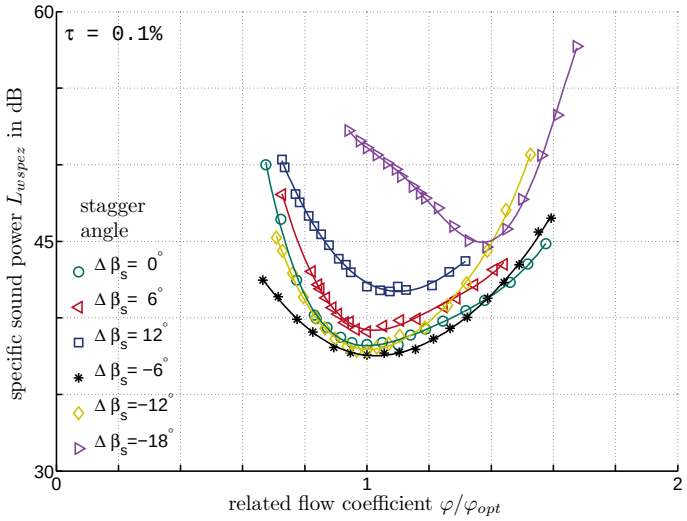

Figure 13. SPECIFIC SOUND POWER VERSUS RELATED FLOW COEFFICIENT FOR $\tau = 0.1\%$

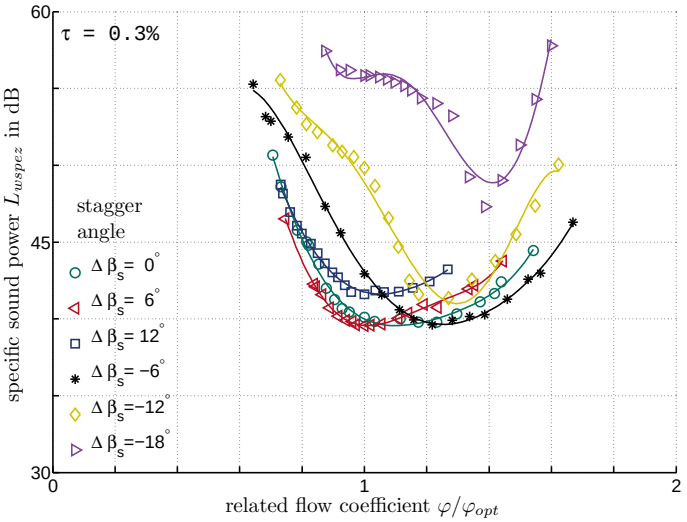

Figure 14. SPECIFIC SOUND POWER VERSUS RELATED FLOW COEFFICIENT FOR $\tau = 0.3\%$

peak can also be found between the second and third harmonic. A variation of the rotational speed assured that these peaks are not the result of resonances of the test rig and remain between the BPF and its first respectively the second and third harmonic. In [5] the tip clearance noise is also located between the BPF and its first two harmonics. The tip clearance noise of the 24-bladed fan in [4] is in front of the BPF. Fig. 11 also affirms the prediction in [5] that this peak also moves to smaller frequencies at lower flow coefficients.

In Fig. 13 the specific sound power is plotted versus φ/φ_{opt} for $\tau = 0.1\%$ for all stagger angles. φ_{opt} is the flow coefficient at $\eta_{sys,max}$. It can be seen that almost all minima of $L_{w,spez}$ match with $\varphi/\varphi_{opt} = 1$. So that for small tip clearances the most aerodynamic efficient operating point equals the quietest operating point. Regarding the value of $L_{w,spez}$ it can be seen that for $\Delta\beta_s < 0°$, with the exception of $\Delta\beta_s = -18°$, the emitted sound at $\varphi/\varphi_{opt} = 1$ is almost equal to the design angle. For bigger tip clearances (Fig. 14) generally a higher level of specific sound power and a slight move towards higher φ/φ_{opt} especially for $\Delta\beta_s < 0°$ is recognized.

Figure 15 shows the difference of the minima in specific sound power versus the tip clearance. The change in $L_{w,spez}$ is referenced on $\tau = 0.1\%$ for every stagger angle. The best fit lines are plotted through $\tau = 0.1\%$ and $\Delta L_{w,spez} = 0$ dB. The trend towards higher $L_{w,spez}$ with an increasing tip clearance can clearly be proven with this plot. It can also be seen that the influence of τ gets maximal for the large negative stagger angles and decreases noticeably for increasing $\Delta\beta_s$. For $\Delta\beta_s = 12°$ and $\tau = 0.8\%$ the difference in the emitted specific sound power is $\Delta L_{w,spez} \approx 1$ dB. For $\Delta\beta_s = -12°$ and $\tau = 0.8\%$ it is nearly ten times as high.

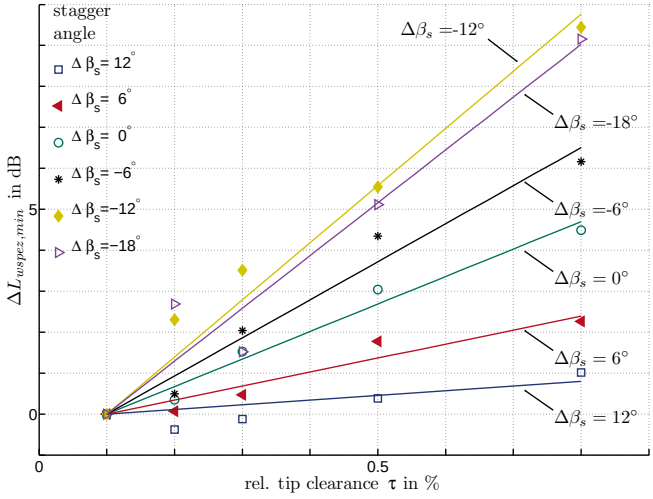

Figure 15. INFLUENCE OF RELATIVE TIP CLEARANCE ON RELATED SPECIFIC SOUND POWER

CONCLUSION

In this experimental study the influence of the tip clearance on the aerodynamic and acoustic characteristics of a fan with skewed blades was measured and analyzed for 30 different fan configurations. A clear trend towards better aerodynamic efficiency and quieter fans with decreasing tip clearances could be shown. The dependence of the influence on the operating point could be proven. It was shown that the tip clearance also has an effect on the stable operating range of this fan. It could also

be pointed out that the influence of the tip clearance on negative $\Delta\beta_s$ is much bigger than on positive $\Delta\beta_s$. The frequency regions where bigger emissions of sound can be found were pointed out as well as the movement of these regions with a change in the tip clearance geometry or in the operating point. It was shown that the aerodynamic influence of the tip clearance on this fan with skewed blades is slightly lower than on the compared standard bladed fans. With the results of this study a calculation of the most efficient design point for aerodynamics as well as acoustics can be made and the advantage can be calculated against the extra manufacturing costs for smaller tip clearances.

REFERENCES

[1] Beiler, M., and Carolus, T., 1999. "Computation and measurement of the flow in axial flow fans with skewed blades". *Journal of Turbomachinery (1999), Vol.121, pp. 59-66.*

[2] Betz, A., 1926. "Über die Vorgänge an den Schaufelenden von Kaplan-Turbinen". *Hydraulische Probleme*, pp. 161–179.

[3] Marcinowski, H., 1958. "Der Einfluß des Laufradspaltes bei leitradlosen frei ausblasenden Axialventilatoren". *Sonderdruck aus Voith Forschung und Konstruktion. Nr. 3.*

[4] Kameier, F., 1993. "Experimentelle Untersuchung zur Entstehung und Minderung des Blattspitzen-Wirbellärms axialer Strömungsmaschinen". PhD thesis, Technische Universität Berlin.

[5] Fukano, T., and Jang, C.-M., 2003. "Tip clearance noise of axial flow fans operating at design and off-design condition". *Journal of Sound and Vibration (2004), Vol.275.*

[6] ISO 5136, 2003. *Acoustics - Determination of sound power radiated into a duct by fans and other air-moving devices - In-duct method.* Berlin, Beuth Verlag.

[7] Karstadt, S., 2008. "Einfluss des Ringspalts auf die akustischen und aerodynamischen Kenndaten eines Ventilators". Diploma thesis, Technische Universität Darmstadt.

[8] Madison, R., 1949. *Fan Engineering (Handbook) 5th ed.* Buffalo Forge, Buffalo, New York.

[9] Jang, C.-M., Sato, D., and Fukano, T., 2004. "Experimental analysis on tip leakage and wake flow in axial flow fan according to flow rates". *Journal of Fluids Engineering (2005), Vol.127, pp. 322-329.*

[10] Longhouse, R., 1978. "Control of tip-vortex noise of axial flow fans by rotating shrouds". *Journal of Sound and Vibration (1978), Vol.58(2), pp. 201-214.*